OTC Paper Number 23715

Improvements in the Detection of Hazardous Sea Ice Features Using Upward Looking Sonar Data

David Fissel, Ed Ross, Keath Borg, Dave Billenness, Anudeep Kanwar, Adam Bard, Dawn Sadowy and Todd Mudge. ASL Environmental Sciences Inc.

This paper was prepared for presentation at the Arctic Technology Conference held in Houston, Texas, USA, 3-5 December 2012.

Abstract

Upward looking sonar (ULS) instruments have been widely used since the mid-1990s to provide accurate measurements of sea ice drafts and ice velocities in support of oil and gas exploration programs in the Arctic Ocean and marginal ice zones. Operated from subsurface moorings located safely below the sea ice canopy, ULS measurements are made continuously at time intervals of 1 or 2 seconds for periods of one year or longer. Modern ULS instruments provide unprecedented horizontal resolution of approximately 1 m of the underside of the sea ice. In this paper we analyses multi-year ULS measurements of sea ice in the Beaufort Sea and off Northeast Greenland.

The analysis results from ULS ice data are used to provide key inputs to the engineering of offshore platform design and ship-based ice management programs required to safely and effectively conduct exploration and production in ice-infested waters.

Improved analysis methods are presented which provide quantitative characterizations separately for highly deformed sea ice features. These features include large individual ice keels and segments of highly concentrated large hummocky (rubbled) ice. Individual large ice keels have the largest ice thickness of up to 20 m or more while large hummocky ice features have greater horizontal scales of 100 to several hundred meters with lesser ice thickness. The detectability and characterization of multi-year ice features in the high resolution ULS ice draft is also presented. In addition, new analysis methods have been developed for detecting episodes of large internal ice pressures based on the cessation of ice motion as revealed from the combined ice draft and ice velocity data sets. The improved analysis techniques have been adapted to work effectively in near-real time applications.

The analysis results provide improved quantitative values for pressure loading of sea ice on offshore platforms and ships. Near real-time analysis results of the ULS data provides improved capabilities in support of ice management operations for offshore drilling.

Introduction

Upward-looking sonar (ULS) instruments have become the primary source of data for high resolution and long duration measurements of sea ice drafts to support engineering requirements for oil and gas exploration projects in Arctic and other ice-infested areas. The data sets provide typical accuracies of 0.05 m for ice draft on a continuous year-long basis; these data attributes allow detailed characterization of keel shapes and other ice features (1). ULS instruments, in the form of ASL's Ice Profiler, have the data capacity for unattended operation for continuous measurement periods of two years, with three year operations possible under some circumstances. When combined with a companion Acoustic Doppler Current Profiler (ADCP) to measure ice velocities, the combined data sets provide horizontal resolution of 1 m or better. The combined ice thicknesses and ice velocities, measured along thousands of kilometers of ice which typically move over each moored ice profiler location, provide important data for establishing metocean design criteria related to oil and gas operations in areas with seasonal or year-round ice cover.

The early versions of ULS instruments for sea ice measurements were developed in the early 1990's (2) for scientific studies of Arctic sea ice. In 1996, the first ULS sea ice oil and gas application was conducted in the Sakhalin exploration area using the ASL Ice Profiler, which was purpose designed for this application by ASL Environmental Sciences Inc. (ASL) and the Institute of Ocean Sciences (IOS) of the Canadian Department of

Fisheries and Oceans through a Joint Industry Program funded by Exxon Neftegas and Sakhalin Energy Investment Co. Since then, well over 100 year-long ULS deployments for oil and gas applications have been conducted with these instruments in the ice infested areas of the northern and southern hemispheres.

The capabilities of the instruments for detailed and accurate representation of the thousands of kilometers of sea ice passing over the moored ULS measurement sites are well established. The processing and analysis of these very large data sets are routinely undertaken using an extensive library of purpose designed software.

For oil and gas engineering requirements there is a particular need the detection and characterization of hazardous sea ice features in these very large ULS data sets. In this paper, we present the basis for the development of algorithms used in the detection and measurement of hazardous ice features. The types of hazardous ice features that are considered are:

1. very thick individual ice keels with thicknesses of 5 to well over 20 m spanning distances of up to 100 m or more;
2. long sections of thick hummocky sea ice spanning greater distances (100 to several hundred meters) but lesser maximum ice drafts than (a) ;
3. occurrences of multi-year ice floes; and
4. episodes of large internal ice pressures based on accurate determination of the cessation of ice motion as revealed from the combined ice draft and ice velocity data sets.

The improved analysis techniques are being adapted to work effectively for both post instrument recovery of full ULS data sets and for near-real time applications. Recommendations are provided for the development of further enhancements to these algorithms.

Upward Looking Sonar Measurements

Instruments

The upward looking sonar instrumentation, consisting of the Ice Profiler Sonar (IPS) and the Acoustic Doppler Current Profiler (ADCP) are designed to be deployed 25 to 60 m below the air water interface from sea floor based moorings (Figure 1) or, in shallower water, from bottom-mounted platforms. As developed in the early 1990's (2) the instrument operated by emitting and detecting surface returns from frequent short pulses (pings) of acoustic energy concentrated in narrow beams (less than 2°). Precise measurements of the delay times between ping emission and reception were converted into ranges separating the instrument's transducer and the ice undersurface. Contemporary data from the instrument's on-board pressure sensor were then combined with atmospheric surface pressure data and estimates of the mean sound speed in the upper water column (obtained from data collected during absences of ice above the instrument) to derive estimates of ice draft from each emitted ping.

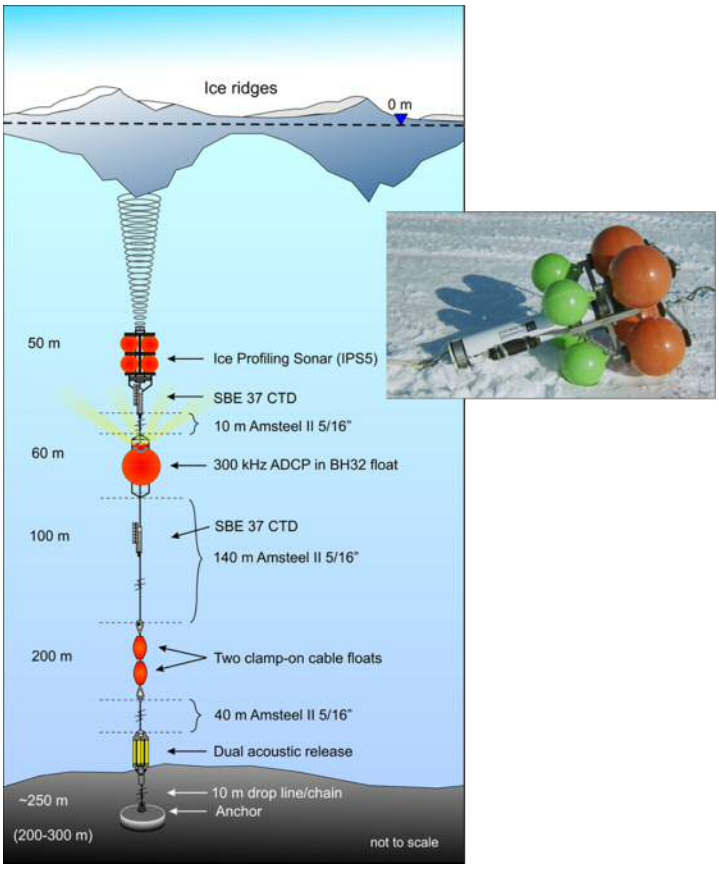

Figure 1. A typical deployment arrangement of an ice profiler and ADCP ice velocity measuring instruments on a single subsurface mooring. In shallow waters the Ice Profiler and ADCP are operated from separate moorings located within 100 m of one another.

Ice Draft Data

When IPS instruments are deployed under moving ice fields and adjacent to upward-looking ADCP (Acoustic Doppler Current Profiler) instruments (Figure 1) with capabilities for extracting ice drift velocity, the obtained data are used to construct two dimensional cross-sections of the ice cover (Figure 2), designated as quasi-spatial profiles (or ice distance series). With careful processing these products depict detailed variations in the depth of the lower ice surface with a horizontal resolution of about 1 m and an accuracy in the vertical of 5-10 cm. Keys to the utility of the technique are its on-board data storage capacity and capabilities for reliable long term un-attended operation in the hostile environments usually associated with ice covered waters. Until recently, principal users of this technology have been polar ocean scientists with interests and concerns regarding climate change (3) and, increasingly, international oil and gas producers with deployments throughout the Arctic Ocean and in sub-polar seas (Figure 3)

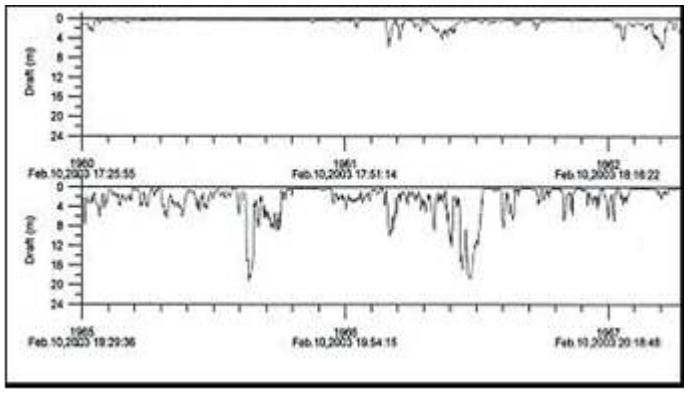

Figure 2. A quasi-spatial profile of an ice cover produced by combining time series draft and ice speed data to produce a product equivalent to the profile of the ice undersurface along a line traced out by all points on the ice which move over the ice profiler instrument during the measurement period. The abscissa is in kilometers, annotated with time of observation.

A new generation of Ice Profiler instruments became available in 2007 (4) which provide enhanced capabilities for sea-ice measurements in the form of more data storage capacity, better resolution and the capability to measure the acoustic backscatter returns beneath and into the ice in addition to the target range to the underside of the sea-ice.

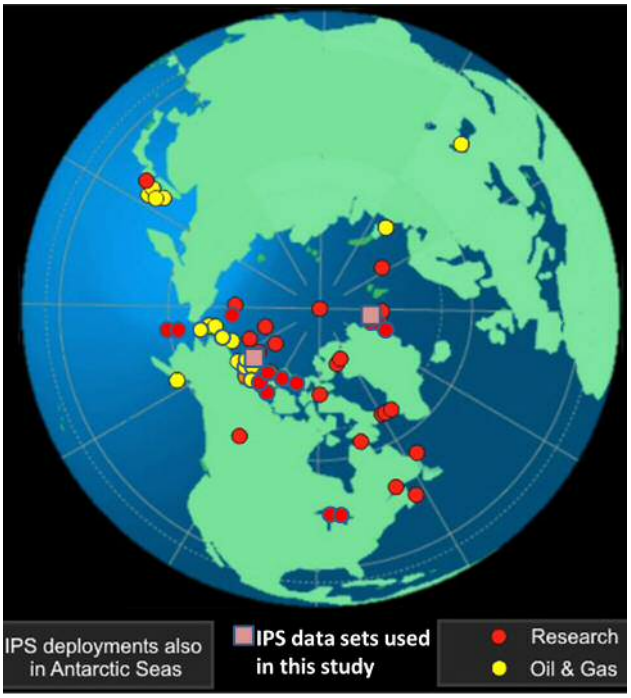

Figure 3. Locations of marine moored ice profiler deployments in the Northern Hemisphere from 1996 to the present. Ice profiler locations for scientific applications are shown by red symbols while oil and gas locations are shown by yellow symbols. The square symbols designate the ULS measurement locations in the Canadian Beaufort Sea and in western Fram Strait used in preparation of this paper.

Large Individual Ice Keels

Methodology

Each large ice keel in the spatial or distance ice data sets is identified from special scanning software applied to the 1.0 meter resolution ice draft spatial series. The algorithm used in identifying large individual ice keels follows the methods described in (5) as Criterion A including user-selected parameters of: a threshold value of the maximum ice draft value that each ice keel must exceed (Start Threshold, values of 5, 8 or 11 m are often used) which starts the search; and the Rayleigh criterion (α= 0.5) and a lower End Threshold (typically set at 2m) which together determine the end of the large ice keel. Once the end of the keel was found, the data points were scanned backwards in the file from the Start Point until the beginning of the keel was found. An example of a large individual ice keel, along with the parameters used by the keel selection algorithm, for forward searches, is shown in Figure 4. More details on the big keel algorithm are available in (6).

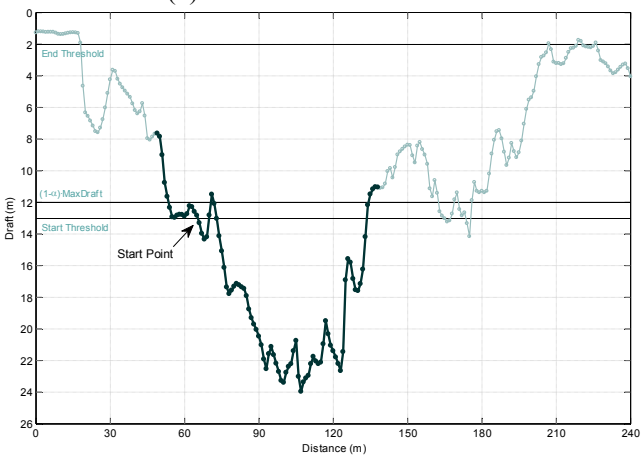

Figure 4. A quasi-spatial profile of an ice cover produced by combining time series draft and ice speed data to produce a product equivalent to the profile of the ice undersurface along a line traced out by all points on the ice which move over the ice profiler instrument during the measurement period. The abscissa is in kilometers, annotated with time of observation. Note that the keel ends (forwards or backwards) if the drafts crossed the End Threshold or if it reversed slope past a threshold given by (1 - α)*Maximum Draft.

Overlapping big keels can also result from the backward search of the next successive keel when a keel with a very large maximum draft value is followed by a keel with a lesser maximum draft value, as long as both exceed the specified Start Threshold value. An example of a combined ice keel feature which includes two originally individual ice keels with some overlap is presented in Figure 5. More details on the methodology, including a description of the software developed to compile a database of all large ice keel features is provided in (6).

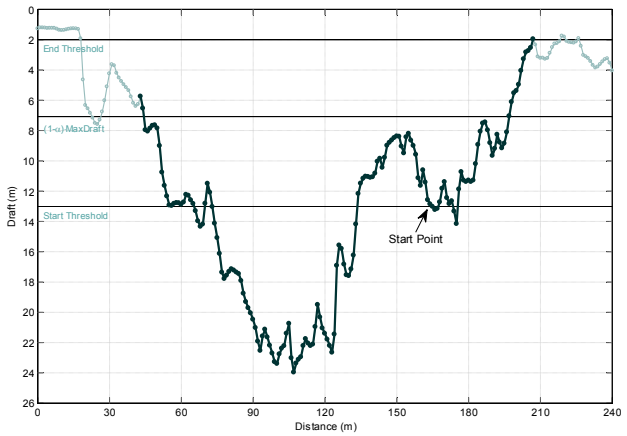

Figure 5. An example of a large keel feature extending from the Start Point beyond the feature shown in Figure 4, which had some overlap with the preceeding keel, resulting in a combined ice keel feature.

Large Ice Keel Results

A statistical compilation of large keel results for a year-long measurement period (2006-2007) on the outer continental shelf of the Canadian Beaufort Sea is provided in (6). For this location - site 2 in (2) over a 12 month period, 5,554 individual large ice keels, exceeding 5 m draft, were identified and extracted from the spatial ice draft data series. The number of large keels for the 8 m and 11 m threshold ice draft value were 1,346 and 335. The maximum measured ice draft was 26.6 m, in May, with ice keel drafts exceeding 15 m occurring from November until the following summer (July). The average width of the large ice keel features were 31.1 m (5 m threshold), 34.7 m (8 m) and 46.2 m (11 m). The maximum monthly width of these large ice keels is typically 100 – 150 m, although a few keels are identified as having widths of over 300 m.

The ice keels having widths of more than 100-200 m are not likely to be singular individual large keels. Instead, they likely include hummocky (rubbled) ice features, which are defined and described later in this paper and/or they may represent composites of two adjoining large individual ice keels possibly comined with hummocky ice. A re-examination of the identified large keel results is also important because the algorithm for the identification of hummocky ice is applied to the spatial data draft data set after removal of the large ice keels; inclusion of hummocky ice in the large keel results would result in missing some episodes of hummocky ice. For these reasons, further investigations of the large keel identification algorithm have been conducted.

The analysis of the large keel algorithm was conducted in two areas: (a) at four locations in the Canadian Beaufort Sea (2009-2011): sites A1 (670 m water depth); F (1010 m); G (690 m), I (75 m) and J (83 m) and (b) two locations on the western side of Fram Strait between NE Greenland Svalbard (2008-2009): site F13 (1000 m) and site F14 (280 m).

The total number of large keels exceeding 100 m in width as computed for Start Threshold values of 5, 8 and 11 m (Table 1) is much larger in the Fram Strait region than in the Canadian Beaufort Sea by a factor of 5.5. The percentage of keels having widths exceeding 100 m is also larger by 50% or more for Fram Strait and the Canadian Beaufort Sea. For the lower Start Threshold values of 5 m, there are many keels exceeding 100 m in width (83 and 770 in each region) which account for 2% and 3.6% of all keels. For the 11 m Start Threshold value the number of keels exceeding 100 m in width is much reduced (10 and 99) but the percentage increases to 10-15%. The effect of not combining overlapping features in the large keel algorithm (see Table 2 in comparison to Table 1) results in an increase in the total number of large keels but a reduction in the percentage of occurrence of keels exceeding 100 m width by 35% for the 5 m ice draft threshold and by 15% for the 11 m ice draft threshold.

Table 1. The total number of identified large keels for Start Thresholds of 5, 8 and 11 m, and the numbers exceeding 100 m in width computed for four sites in the Canadian Beaufort Sea and two sites in Fram Strait.

			With overlapping keels combined		
Start Threshold (m)	Areas:	# of site-years	Total # keels	# > 100m width	% > 100m width
5	Beaufort Sea: Average	7	4484	83	1.9
	Fram Strait: Average	2	21323	770	3.6
8	Beaufort Sea: Average	7	1082	29	2.7
	Fram Strait: Average	2	6369	260	4.1
11	Beaufort Sea: Average	7	273	10	10.5
	Fram Strait: Average	2	1719	99	15.5
Notes:	Canadian Beaufort Sea: 4 sites (A1, F, I and J) over 2 years 2009-2011				
	Fram Strait - NE Greenland: 2 sites (F13 and F14) in 1 year (2008-2009)				

Table 2. The total number of identified large keels when the ice keel algorithm does not include combined keels arising from overlaps (see Table 1 for details)

			Without combined keels from overlaps		
Start Threshold	Areas:	# of site-years	Total # keels	# > 100m width	% > 100m width
5	Beaufort Sea: Average	7	4890	51	1.0
	Fram Strait: Average	2	23788	528	2.2
8	Beaufort Sea: Average	7	1144	21	1.8
	Fram Strait: Average	2	6752	207	3.1
11	Beaufort Sea: Average	7	284	8	7.2
	Fram Strait: Average	2	1781	87	12.1

In reviewing the ice segments that are classified as a single large ice keel, a basic parameter to consider is the aspect ratio of the total width to the maximum draft of each ice feature. A very large value of this aspect ratio could be an indication of identified large keels that are not realistically classified. To investigate this further, the distribution of the width to maximum draft aspect ratio was computed for the Beaufort Sea and Fram Strait data sets. As expected, the vast majority of the classified large ice keels have aspect ratios between 3 and 10. The aspect ratios computed for the 5 m large keels (Figure 6), indicate that cases occur with aspect ratios much greater than 10 ranging up to 30-50 or more, especially for large keels having widths exceeding 100 m. The number of

large aspect ratios is greater for the Fram Strait data sets that for the Canadian Beaufort Sea data sets. A manual review of these large keel episodes with high aspect ratios for wide keels indicates that a small, but non-negligible number of hummocky ice events are being misinterpreted as large keels in some cases.

For the 11 m large keels, the occurrences of aspect ratios exceeding 10 are much reduced (Figure 7). The number of outlier aspect ratios is limited to only a few cases for all data sets considered. The maximum keel width for the 11 m threshold is reduced from that of the 5 m threshold for large keels. A manual review of the large ice keel episodes, having large aspect ratios indicate that these episodes are not due to hummocky ice, but rather arise from very wide single ice features, especially for Fram Strait, or less often, juxtapositions of two or more large keels.

Based on the analysis results of large keels as presented above, the large keel algorithm requires improvements, in particular, for use with a Start Threshold of 5 m, while it is reasonably effective for 11 m threshold values.

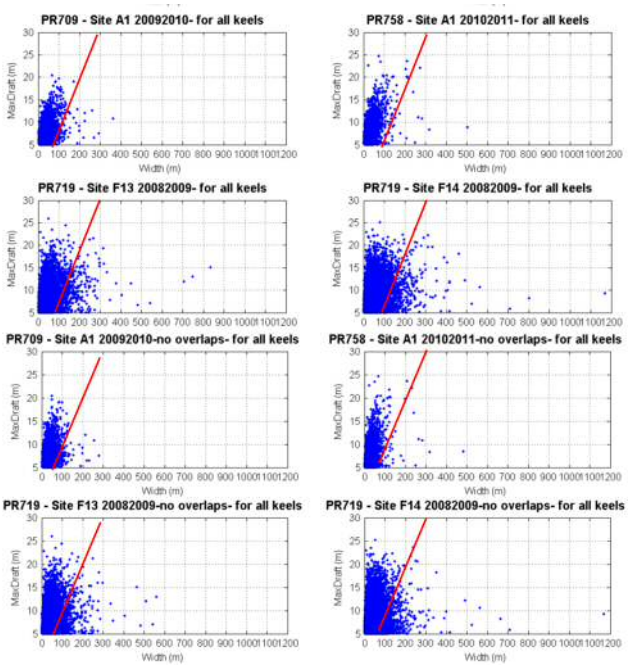

Figure 6. Plots of the aspect ratio of 5 m large keel width to the maximum ice draft for year-long data sets at site A1 in the Canadian Beaufort Sea and at sites F13 and F14 in Fram Strait. The upper four panels are computed from the large keel algorithm while the lower four panels are for the modified algorithm with no combinations of the large ice keel episodes due to overlaps. The red line represents the aspect ratio of 10.

Hummocky Ice Features

Methodology

Hummocky (sometimes referred as ice rubble fields) sea ice represents a different type of deformation of first year sea ice from the large ice keel features described above (sometimes referred to as pressure ridges). Distinctions between hummocky and large ice keels are based on the underlying deformation mechanism for each ice type: hummocky ice originated primarily from compressive events which force adjacent floes to ride up or slide over each other while ridged ice tends to arise from more drastic events in which smaller ice pieces are crushed and turned so that their original planes are oriented well off the vertical direction to produce combined deformed ice features which are larger in the vertical dimension and have distinct sides (1).

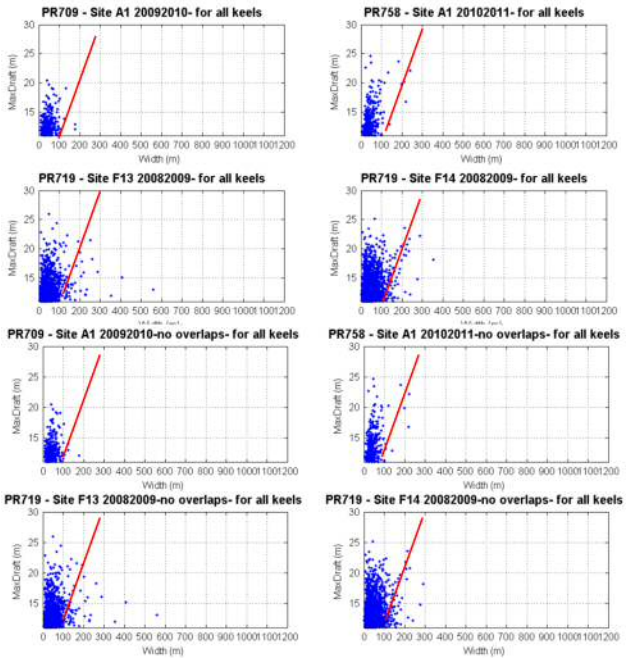

Figure 7. Plots of the aspect ratio of the 11 m large keel width to the maximum ice draft for year-long data sets at site A1 in the Canadian Beaufort Sea and at sites F13 and F14 in Fram Strait using the same format as Figure 8.

Automated methods for detecting hummocky ice were derived from analysis of several ice profiler sonar (IPS) data of sets from the Canadian Beaufort Sea as described in (6). The spatial ice draft series were examined for continuous segments of hummocky ice, initially identified by satisfying four criteria:

1. The minimum draft is no lower than 1m
2. The segment maintains this minimum draft for at least 100m in distance
3. The 50th percentile draft is at least 2.5 m
4. The segments are free of any keels already identified in the 5m large keel database.

Based on the segment identified through these criteria, a method based on statistical parameters was developed (6) to automatically classify likely episodes of hummocky ice, as follows:

$\gamma > 2$: The probability that the segment fits the description of hummocky ice is very high. In these cases the standard deviation is comparatively low, so the ice segment would tend to be fairly level.

$\gamma < 1$: There are large keels present in the segment and the probability that it is hummocky ice is low. The sizes

of the keels are quite large compared to the 50th percentile value, but the standard deviation is also high, resulting in a low gamma.

where the statistical parameter, γ is the 90th percentile over the 50th percentile value of the ice draft values, divided by the standard deviation.

These limiting cases were shown to work reasonably well as a first approximation. For intermediate values, a histogram of the draft records in the segment needs to be examined before determining whether the segment is hummocky ice. These segments could be broken down as:

$1.5< \gamma <2$: Usually hummocky ice, but could also be a small keel (less than keel database threshold) surrounded by level ice of a relatively similar value;

$1.0< \gamma <1.5$: Not usually hummocky ice, keels are much larger than median or surrounding values.

Hummocky Ice Keel Results

The algorithm for classification of hummocky ice has now been extended to ice profiler (IPS) data sets from Fram Strait (Figure 3). The amount of hummocky ice detected was found to be very sensitive to the removal of the 5 m large keels prior to applying the algorithm. For site F14, the amount of hummocky ice detected (using $\gamma >$ 1.5) was limited to 120 km, which was much less than the 850 km total distance of 5 m large keel episodes. However, when the hummocky ice algorithm was applied after the removal of 8m large ice keels, which had a total of 289 km in distance, the total distance of the hummocky ice segments increased to 819 km. This amounts to an increase by a factor of 7 in the distance of hummocky ice detected for the same data set after using different approaches to remove large keels. For the case of removal of the 8 m ice keels, the total number of hummocky ice segments numbered 2,222 corresponding to an average width of each segment of 368 m. In this case, an inspection of the resulting hummocky ice episodes revealed that the results were generally reasonable.

The hummocky ice classification algorithim was run with the standard settings (1m draft for 100m or more, $\gamma > 1.5$) but without the removal of any ice keels. Figure 8 presents examples of data segments which have an appearance consistent with that expected for hummocky ice. These segments would have been excluded if the 5 m keel constraint was applied but not if the 8 m ice drafts were removed. Further investigations are required for determining the optimal methods for pre-conditioning the ice draft distance data to which the hummocky ice classification algorithm is applied.

Multi-Yea Ice Floes

Methodology

While first year ice is the dominant ice type in the Arctic Ocean, some of the sea ice is older having survived at least one summer. Old ice has two categories: second year ice and multi-year ice. As sea ice ages from year to year, its physical properties change (7). The salinity is reduced as the brine channels are evacuated and frozen over. The hardness of the ice increases and it yields less to external objects such as ships making passage through the ice, leading to the more hazardous nature of encounters with this multi-year ice. The topography of the ice also changes as it tends to becomes smoother on its top and bottom sides due to partial melting in summer leading to smoothing of its rough topographic features.

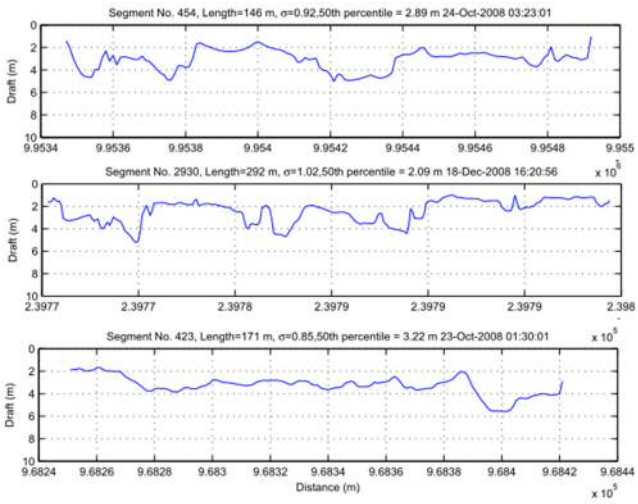

Figure 8. Example plots of three ice draft segments classified as hummocky ice by the algorithm on the site F14 ice draft distance data without any prior removal of large ice keels.

Detection of old (second- or multi-year) ice from upward looking sonar data sets is challenging. There are two basic approaches that have been considered (6):

1. Analysis of the shape of the leading edge of the acoustic backscatter return realized from the ice return on each individual acoustic ping.
2. Determination of the roughness scales of the underside of the sea-ice to differentiate between the smoother old ice from the rougher first year ice which involves analysis of ice drafts from several successive pings to determine a bottom roughness scale;

Multi-Year Ice Results

The methods previously developed for the available ice profiler sonar (IPS) data sets on the Canadian Beaufort Sea shelf region were extended to the deeper slope waters of the Canadian Beaufort Sea and data sets in Fram Strait (Figure 3). Multi-year ice occurs rarely in the shallower waters of the Beaufort Sea but is found more frequently in the deeper waters closer to Arctic Ocean pack ice. Fram Strait has even more multi-year ice because of the Trans-Polar Drift Current of the Arctic Ocean which transports thick and older ice out of the Arctic Ocean into the North Atlantic Ocean through Fram Strait.

Distinguishing between old and first year ice on the basis of the leading edge of the acoustic return for an individual acoustic ping is based on the concept that the harder and more compact old ice will have a steeper rate of increase

in the leading edge of the acoustic returns on encountering the underside of the ice. An example of two different rise times for acoustic pings is given in Figure 9.

IPS profiles (acoustic backscatter returns vs. time from a single acoustic ping) from the 2009-2010 deployment at Sites F and G were selected based on a criteria designed to ensure representative responses from the instrument. Parameters from selected profiles were examined for evidence of multi-year ice from weeks where Canadian Ice Service (CIS) weekly ice charts indicated its presence in the summer of 2009, and the results were compared to control data at the same measurement site from weeks where the ice charts indicated no presence of multi-year ice (spring of 2010). Unfortunately, the IPS profile measurements were not available in the Fram Strait data sets.

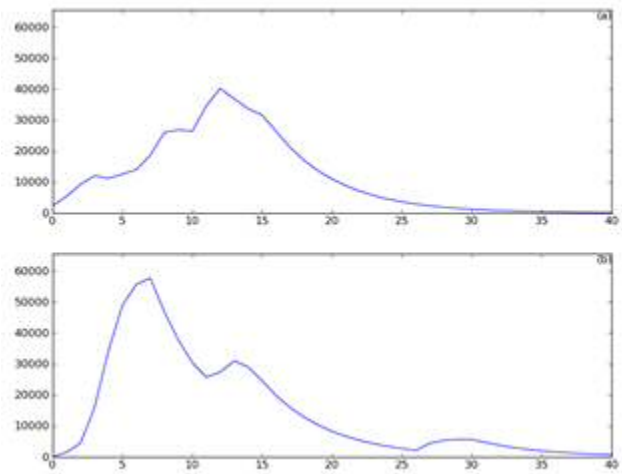

Figure 9. The acoustic backscatter return (as instrument analog to digitlal (A/D) counts) is shown for individual pings that may represent two different sea ice types: (a) from first year ice and (b) from old ice. The x-axis is in A/D samples count numbers, starting from the initial rise of the return for the ice target. One A/D sample respresents 15.6 micro-seconds.

To ensure that the profiles examined were representative of the underside of the sea ice feature for the ice draft values in the insonified area were reasonably consistent rather than along the side or other areas of large changes in ice drafts over short distances comparable to the insonified area, the analysed data was pre-conditioned. The conditions were designed to include only ice of sufficient draft, with relatively "flat" features. The profiles were first qualified to have occurred at a draft of at least 3 meters. In addition, the distance ice draft series was windowed to those values occurring within the sonar beam of the IPS5 instrument. The window size is $2d \cdot \tan(\theta)$, where θ is the beam angle of the IPS5, nominally 1.8 degrees, and d is the instrument depth below the underside of the ice. A linear regression of the windowed draft series was taken, and profiles were further selected by the slope of this regression. A maximum absolute slope of 0.1 (Δdraft / distance) was required. Finally, any profile where the difference between the maximum and minimum draft in the selected window was greater than 0.4m, was rejected.

The qualified profiles were combined by week, and the mean and standard deviation values of the persistence, maximum amplitude, and corrected slope were computed. The persistence value is the elapsed time that the amplitude values exceed a threshold level (typically 10,000 counts). The corrected slope is computed as the change in amplitude from the threshold value to the maximum value on the leading edge of the strong return from the underside of the ice divided by the time duration.

The results of the analysis of the profile data sets are presented in Table 3. It is seen that the slopes of the leading edge of the acoustic returns from the periods when old ice is present is approximately 35-40% larger than when no old ice is reported. When old ice was reported, the ice charts indicted that thick first year ice was also present at up to 50% of the total ice concentrations. Therefore, in the increase in the slope of the leading edge ice returns may actually be larger than indicated in the results of Table 9. Note that there is a large amount of variability in the corrected slope, and other values computed for each week. Therefore, the detection of old ice results from the realization of many profile pings rather than any single ping.

Table 3: A comparision of the acoustic returns of the leading edge of the ice returns from individual pings for site F and G in the Canadian Beaufort Sea in 2009-2010 for weekly periods when old ice was reported to present or not to be present from ice charts.

Date	Percent Old Ice Present	# of Qualified Pings	Persistence (micro-s)		Amplitude (A/D counts)		Corrected Slope (counts/micro-sec)	
Site F			Mean	Std.Dev.	Mean	Std.Dev.	Mean	Std.Dev.
27/07/2009	>50%	587	32.9	13.2	54,408	16,423	534	277
03/08/2009	>50%	188	37.5	13.7	59,850	12,007	551	234
10/08/2009	>50%	76	39.1	14.0	60,348	12,395	554	218
17/08/2009	>50%	148	42.5	16.0	59,659	11,869	521	219
24/08/2009	>50%	57	32.9	12.3	56,403	15,867	531	281
31/08/2009	>50%	53	39.2	15.1	61,100	10,243	584	243
Totals with old ice	**Average**	**1109**	**37.3**	**14.1**	**58,628**	**13,134**	**546**	**245**
03/05/2010	none	62	22.4	10.3	37,324	19,878	366	298
10/05/2010	none	80	22.4	11.3	39,720	19,442	376	306
17/05/2010	none	77	20.9	9.9	43,123	21,857	456	325
24/05/2010	none	102	24.4	11.1	43,192	19,772	414	317
Totals without old ice	**Average**	**321**	**22.5**	**10.6**	**40,840**	**20,237**	**403**	**311**
Site G								
27/07/2009	>50%	177	16.7	7.7	45,204	20,977	462	300
03/08/2009	>50%	44	20.6	7.8	52,013	18,667	516	302
10/08/2009	>50%	29	21.8	10.5	55,588	19,303	548	308
17/08/2009	>50%	64	17.7	7.8	50,650	20,275	521	289
Totals with old ice	**Average**	**314**	**19.2**	**8.4**	**50,863**	**19,806**	**512**	**300**
03/05/2010	none	158	6.2	5.9	17,878	17,475	191	239
10/05/2010	none	88	9.8	6.2	31,643	23,138	354	313
17/05/2010	none	108	10.0	6.1	37,228	25,036	443	364
24/05/2010	none	82	11.8	6.5	40,605	24,676	472	363
Totals without old ice	**Average**	**436**	**9.4**	**6.2**	**31,839**	**22,581**	**365**	**320**

Analysis of the second method based on the smoothness characteristics of ice draft distance segments is underway. The data sets being used in this analysis are from the offshore Beaufort Sea sites as well as the Fram Strait data sets. The initial criteria for selecting the data segments is

for relatively constant ice drafts (to avoid the edges of ice floes) with ice drafts in the range of 3 to 10 m, which is expected to encompass most old ice features.

Detection of Internal Ice Stress Events Using Ice Velocity

Episodes of internal ice stress are important for shipping and fixed structures operating in very highly concentrated sea ice due to the potentially large force that the sea ice can exert on the platform. Measured ice velocities can provide an indication of internal ice stress when ice motion ceases while the winds and ocean currents should be resulting in sea ice motion.

Methodology

The direct measurement of ice velocities using Teledyne RDI ADCP instruments equipped with the "bottom tracking" have been demonstrated to effectively track ice velocities (1,8). The TRDI –ADCP instruments provide ice velocities with a random error of typically ±1.0 cm/s over measurement intervals of 15-30 minutes. Because of this random error, it is not possible to distinguish between essentially stationary sea ice having speeds of less than 0.01 cm/s (movement of 10 m over one day) and very small sea ice movements in the range of 0.01 to 0.1 cm/s. During times of very low ADCP ice velocities, the simultaneous measurements of time and spatial series can be used to determine if the ice is actually stationary, corresponding to a constant ice draft value over periods of hours or longer or if the ice is moving very slowly. Software has been developed to iteratively display and examine the ice time and distance series and the ice velocity magnitude (speed) allowing adjustments to the latter quantity until a consistent representation is realized in both ice drafts and ice speeds. An example of such an adjustment is shown in Figure 10.

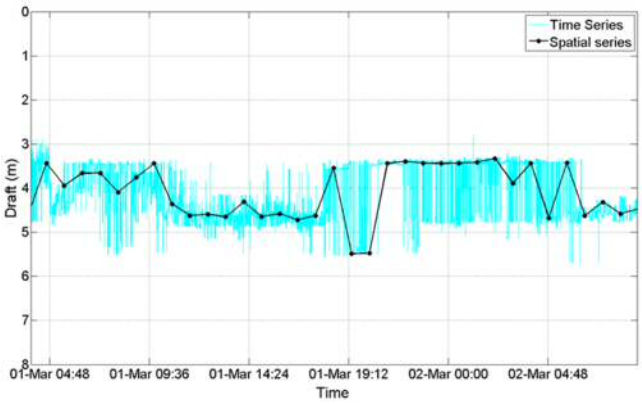

Figure 10. An example of a very slow motion period at Site A. The black line represents the spatial series with each point separated by 2.2 m. This event spans several days (several thousand points in the IPS time series), however it is only represented by a few points in the spatial series by estimating a very small constant ice velocity over the entire event.

Stationary Ice Events indicative of Internal Ice Stress

The offshore Canadian Beaufort Sea data sets are being reviewed to determine the frequency of occurrence of zero or very low ice speeds, as an indicator of internal ice stress. High occurrences of very low ice speeds were obtained in winter and early spring, especially at sites I and J in 75 m and 83 m water depth, respectively, on the outer portion of the Canadian Beaufort Sea shelf. The percent occurrences of zero and low ice speeds for site I in 2009-2010 am presented in Table 4. For the months of February to May inclusive, very low ice speeds occur from 20 to 66% of the time. The occurrence of zero ice speeds represents at least one-half of the very low ice speeds in these months. Very low ice speeds can occur through early summer when ice concentrations remain very high as was the case for the last week of July 2009 when ice speeds were less than 1 cm/s 62% of the time, including 18% occurences of zero ice speeds.

Table 4. A tabulation of the frequency of occurrence of very low ice speeds at site I in the Canadian Beaufort Sea, 2009-2010, as determined fromt the combined use of TRDI-ADCP ice velocity and ice draft data sets.

	Site I				
Month	# points	# pts < 1 cm/s	% 1 cm/s	# zero points	% zero points
Jul-09	816	497	60.9	149	18.3
Aug-09	1184	4	0.3	0	0
Sep-09	0	0	-	0	-
Oct-09	604	0	0	0	0
Nov-09	2880	312	10.8	225	7.8
Dec-10	2976	34	1.1	1	0
Jan-10	2976	684	23	198	6.7
Feb-10	2688	582	21.7	516	19.2
Mar-10	2976	1968	66.1	1245	41.8
Apr-10	2880	990	34.4	458	15.9
May-10	2976	593	19.9	573	19.3
Jun-10	535	0	0	0	0
Jul-10	0	0	0	0	0
Aug-10	0	0	0	0	0
Sep-10					
Total	23491	5664	24.1	3365	14.3

An example of episodes of very low ice speeds for site I in March 2011 is shown in Figure 11. The importance of wind forcing is clearly evident in the ice velocities. When the wind blows from the west, the ice motion slows and reaches zero speeds after a time lag of approximately one day. The cessation of ice motion is due to the onshore movement of the ice in response to westerly wind forcing associated with the Coriolis force and the highly concentrated ice conditions present on the Beaufort Sea shelf. Ice movement reaches zero speeds under wind speeds of up to 10 m/s and current speeds of up to 15 cm/s.

Episodes of internal ice stress can be identified by very

low or zero ice speeds in the presence of non-zero wind and ocean current speeds. To develop estimates of the magnitude of the internal ice stress, the combined forcing of the wind and near-surface ocean currents expressed as momentum flux values can provide a lower bound for estimation of the internal ice stress.

Summary and Conclusions

ULS ice measurements obtained from year-long moored Ice Profiling Sonar (IPS) and ADCP instruments can be used to identify and quantify episodes of potentially hazardous ice events. The knowledge and understanding of such events contributes to developing engineering solutions for offshore platform design and ship-based ice management programs, as required to safely and effectively conduct exploration and production in ice-infested waters.

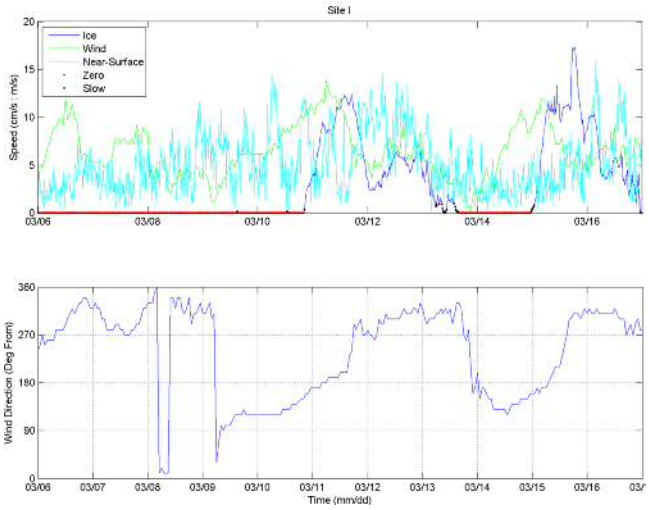

Figure 11. The ice velocities at site I from March 6 – 16, 2011 (in cm/s) as well as the ADCP measured near-surface ocean currents (in cm/s) and the wind speeds (in m/s). Also, plotted in the lower panel is the wind direction in degrees clockwise from, e.g. 90 is a wind from the east).

In recent years, algorithms have been developed for the detection and classification of hazardous ice features using upward-looking sonar. By combining acoustic devices that measure continuous, high resolution keel depths and ice velocities, a variety of hazards are identifiable, including: identification of individual large ice keels; episodes of large hummocky sea ice; occurrences of multi-year ice floes; and detection of episodes of large internal ice stress sufficient to stop ice motion.

Further methodology and software development is required, with development presently underway to address some remaining issues. The distinction between large singular ice keels (pressure ridge) and hummocky (rbbled) ice requires more study, especially under the high ice concentrations and relatively large mean ice drafts prevalent off North East Greenland in Fram Strait. The present methods work reasonably well for the large ice keels with ice drafts exceeding 8 to 11 m or more but improvements are need for identifying large ice keels of 5 to 7 m because presently some of the identified large ice keels with widths of 50-100 m or more are being confused with hummocky ice features. For the large draft 11 m keels, occurrences of keel widths of 100 to over 300 m do occur.

The detection of episodes of old ice, including multi-year ice, appears to be possible based on the shape of the leading edge of the acoustic returns from the underside of the sea ice, if special profiling pings are measured (profile pings are an optional operational mode of the IPS instrument). More study of this detection method is required by obtaining IPS data sets using profile pings in which old ice is prevalent and through better independent indications of the presence of old ice than those provided by weekly sea ice charts. Another method of detection of old ice is being investigated based on developing algorithms to determine the smoothness of the underside of ice floes with drafts exceeding 3 m. Old ice floes are expected to be smoother than deformed first year ice over the same range of ice draft values.

Using the combined measurements of ADCP ice velocities and high resolution IPS ice draft time and distance series, it is possible to detect ice speeds much less than 1 cm/s, to essentially zero ice speeds. Based on these data, the cessation of ice movement can be detected under very high concentrations and sizeable wind and current forcing. It may be possible to estimate the lower bound of the internal ice stress for episodes of zero ice speeds based on the computed magnitude of the momentum fluxes (stress) exerted by the measured wind and near-surface ocean currents.

Acknowledgements

The requirements for the methods and software described in this paper have been provided by our scientific and engineering colleagues with the offshore oil and gas companies and with the Institute of Ocean Sciences of the Canadian Department of Fisheries and Oceans (Dr. H. Melling) and the Norwegian Polar Institute (Dr. E. Hansen). The latter two organizations and ExxonMobil Upstream Research (Dr. D. Matskevitch) provided access to data sets that were instrumental to the development of methods and software presented in this paper.

References

1. Fissel, D.B, Marko, J.R. and Melling, H., "Advances in Marine Ice Profiling for Oil and Gas Applications," *Proceedings of the Icetech 2008 Conference,* July 2008.
2. Melling, H., Johnston, P.H. and Reidel, D.L., "Measurements of the Underside Topography of Sea Ice by Moored Subsea Sonar*," J. Atmospheric and Ocean Technology*, 12: 589-602, 1995.
3. Fissel, D.B., J.R. Marko and H. Melling. Advances in upward looking sonar technology for studying the processes of change in Arctic Ocean ice climate. *Journal of Operational*

Oceanography: 1(1), 9-18, 2008
4. Fissel, D.B., Marko, J.R., Ross, E., Chave, R.A. and J. Egan. Improvements in upward looking sonar-based sea ice measurements: a case study for 2007 ice features in Northumberland Strait, Canada, in Proceedings of Oceans 2007 Conference, Vancouver, B.C., Canada, 6p. IEEE Press, 2007.
5. Vaudrey, K.,1985-86 Ice Motion measurements in Camden Bay, AOGA Project 328, Vaudrey & Associates, Inc. San Luis Obispo, CA, 1987
6. Fissel, D.B, Kanwar, A,, Borg, K., Mudge, T., Marko, J. and Bard, A., "Automated Detection of Hazardous Sea Ice Features from Upward Looking Sonar Data," Paper No. 150, Proceedings of the Icetech 2010 Conference, September 2010.
7. Wadhams, P., Ice in the Ocean. *Gordon and Breach Science Publishers*, Amsterdam, The Netherlands. 351 p, 2000.
8. Belliveau, D.J., G.L. Bugden, B.M. Eid and C.J. Calnan. Sea ice velocity measurements by upward-looking Doppler current profilers. *J. Atmos. Oceanic Technology,* 7(4): 596-602, 1990.